

Effect of Monsoon Wind to Current in East Coast of the Gulf of Thailand

Pongsit Polsomboon^{1,2*}, Anurak Sriariyawat^{1,2}

¹ Department of Water Resources Engineering, Faculty of Engineering, Chulalongkorn University
Bangkok, 10330, Thailand

² Research Unit on Technology for Oil Spill and Contamination Management
Chulalongkorn University, Bangkok, 10330, Thailand

*E-mail: Pongsit.polsomboon@gmail.com

Abstract: From 1997 to 2013, there were 11 huge oil spill events occurred in Gulf of Thailand. Therefore, Pollution Control Department (2010) had classified oil spill risk zones by the impacts to the coastal area. East Coast of the Gulf of Thailand where were the sites of industrial estates are the highest risk zone. The circulation pattern will help to investigate oil spill after being release into the system. The main factor of current was tide. But the Monsoons wind also affects the current speed and direction of seawater. The objective of this study was to investigate the influence of wind and tidal to current circulation in East Coast of the Gulf of Thailand. The water level from the tidal model was calibrated by predicted tidal level at stations of Hydrographics Department, while the water level from coupled wind-tidal model was verified with observed data from the tide gauge of Port Authority of Thailand. To identify the major effects on current, the influence of wind and tidal would be investigated in terms of magnitude and direction. Wind is the major effect to the circulation in almost stations in the Upper Gulf of Thailand, while there were some areas that the circulation are influenced by both tidal and wind. This would be useful for revealed seasonal variation in circulation patterns and predicted of possible oil spill in future in East Coast of the Gulf of Thailand at different tide and wind conditions.

Keywords: Tidal Current, Wave Current, Gulf of Thailand, Delft3d model

1. Introduction

Oil spill causes serious problems not only to the environment, but also the tourism and economic of Thailand. There were 11 huge oil spill events occurred in Gulf of Thailand from 2017 to 2013. Therefore, Pollution Control Department (2010) had classified oil spill risk zones in Thailand by the level of risk and the severity of impacts of oil spill into the 4 zones as presented in Figure 1. The zone 1, East Coast of the

Gulf of Thailand where is the sites of industrial estates are the highest risk zone. The Chao Phraya River mouth to the Bangkok port is zone 2 (the higher risk zone). West coast of the Gulf of Thailand and the Andaman Sea in zone 3 are the high risk zone. The other specified in the three zones above are zone 4 (the low risk zone).

For managing the oil spill problem after it released into the system, the behavior of circulation pattern in

the Gulf of Thailand is an important knowledge to specify the locations and procedures for capturing the oil spill. Many researches indicated that the tidal and wind are the main components of the current in the Gulf of Thailand. Some previous researchers pointed out the tidal currents play a dominant role of the current in the Gulf of Thailand (Robinson, 1974; Hydrographic Department, 1995; Choi et al., 1996; Yanagi et al., 1997; and Buranpratheprat and Bunpapong, 1998), while Yanagi and Takao (1998), and Siripong (1984) found that the tidal currents contributed a little in term of the net circulation. The predominant monsoon winds caused eddied, mixing and the exchange of water mass in the Gulf of Thailand. Therefore, this study aimed to investigate the influence of wind and tidal to current circulation in East Coast of the Gulf of Thailand.

The study results would be useful for the revealed seasonal variation in circulation patterns and predicted of possible oil spill in future in the high risk zone of Gulf of Thailand at different tide and wind conditions.

2. Methodology

This study used Delft3D model for simulate circulation from tidal and coupled wind-tidal in the Gulf of Thailand. The tidal constituents are applied to compute tide and tidal current. The wind driven currents were simulated using SWAN model. Comparison the results of current from tidal model and coupled wind-tidal model that used to evaluate effect of wave and tidal on current.

2.1 Study area

The Gulf of Thailand is a shallow inlet in the western part of the South China and Eastern Archipelagic Seas, a marginal body of water in the western Pacific Ocean. The area covers from longitude 99° E to 105.5° E and for latitude form 6° N to 14° N as shown in Figure 1. The gulf is around

800 km long and up to 560 km wide, has a surface area of 320,000 km² and is surrounded on the north, west and southwest by Thailand, on the northeast by Cambodia and Vietnam. The South China Sea is to the southeast. (Department of Mineral Resources, 2012)

The hourly predicted water level data at different tide gauges along the coast of the Gulf were forecasted at Sattahip (SHT), Ko Sichang (SCT), Bangkok Bar (BBT), Tachin (TCT), Hua Hin (HHT), Ko Lak (KLT) and Chumporn (CPT) stations from the Hydrographic Department, Royal Thai Navy. These data were used for calibration and validation of Delft3D model (See Figure 1).

The significant wave height were collected at oceanographic buoy stations, Ko Change (KCB), Rayong (RYB), Ko Sichang (SCB), Huahin (HHB), Phetchaburi (PCB), Songkhla (CPB), Ko Tao (KTB) and Nakhonsitamarat (NKB) stations from GISTDA. These data were used to calibrate and verify the performance of SWAN model (See Fig. 1).

The measurements of water level at Bangkok Bar (BBT) station from the tide gauge of Port Authority of Thailand were used to verify with the water level from coupled wind-tidal model.

2.2 Delft3D

Delft3D-Flow developed by Deltares (2014) was used to calculate non-steady flow and transport phenomena in two (depth-averaged) or three dimensions. Only 2D-depth averaged was used to simulate in this study. Therefore, the equations of Delft3D are consist of horizontal momentum equations, continuity equation, transport equation, and a turbulence closure model. The vertical momentum equation is reduced to the hydrostatic.

$$\frac{\partial u}{\partial t} + u \frac{\partial u}{\partial x} + v \frac{\partial u}{\partial y} - f v = -\frac{1}{\rho_0} P_x + F_x + M_x \quad (1)$$

$$\frac{\partial v}{\partial t} + u \frac{\partial v}{\partial x} + v \frac{\partial v}{\partial y} - f u = -\frac{1}{\rho_0} P_y + F_y + M_y \quad (2)$$

$$\frac{\partial P}{\partial \sigma} = -\rho gh \quad (3)$$

Where u and v are the horizontal velocity components, f is the Coriolis parameter, ρ_0 is the water density, P_x and P_y are the horizontal pressure terms from Boussinesq assumption, F_x and F_y are the horizontal Reynold's stresses which determined using the eddy viscosity concept, M_x and M_y are external sources or sinks of momentum terms, g is the acceleration of gravity and σ is the water level.

The equations used in the flow model are based on the shallow water equations. To solve the unsteady shallow water equations, an Alternating Direction

Implicit (ADI) method is applied as the standard time integration method in which time step is based on the Courant number. The Courant number exceeds the value of 10 will generate instability and inaccuracy in the model computation.

$$CFL = 2\Delta t \sqrt{gH \left(\frac{1}{\Delta x^2} + \frac{1}{\Delta y^2} \right)} < 4\sqrt{2} \quad (4)$$

where CFL is Courant-Friedrichs-Lewy condition, g is the acceleration of gravity, H is the water depth and Δx and Δy are the grid spacing in x , and y direction.

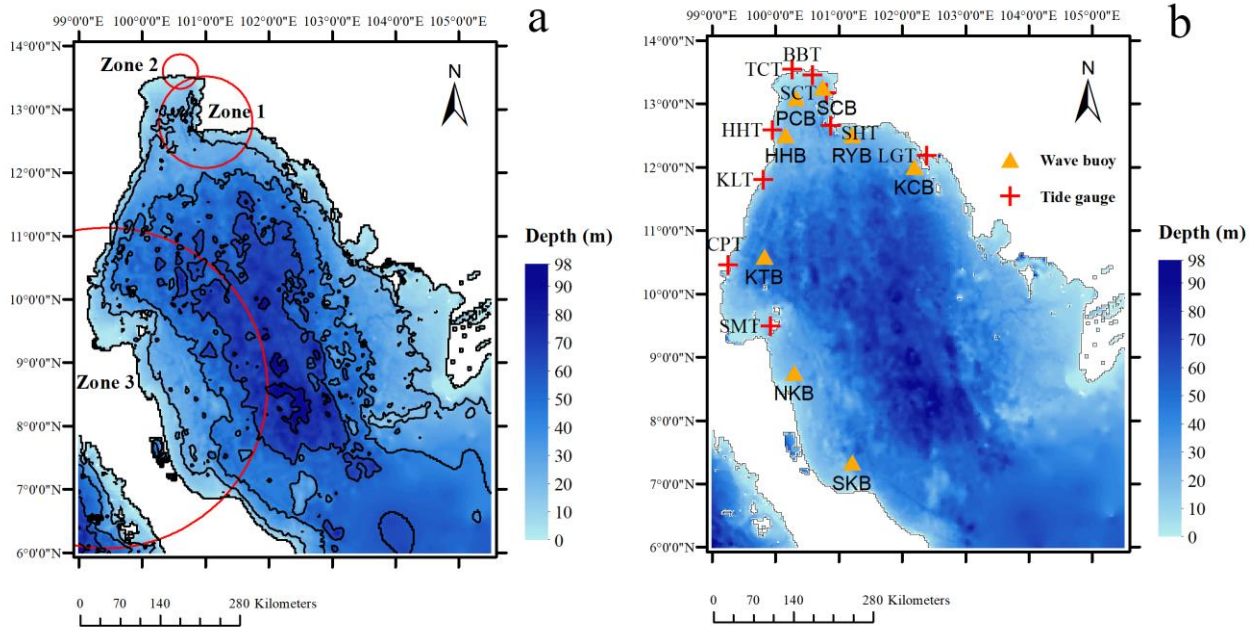


Fig. 1. Oil spill risk zone in the Gulf of Thailand a) and oceanographic stations b).

2.2.1 Model Setup

Grid domain

The curvilinear grid system of Delft3D is developed with 1 kilometer resolution. The open boundary was assigned to be a straight line between Ko Samui and Laem Ngop station.

The bathymetry data is obtained from GEPCO (General Bathymetric Chart of the Oceans) with resolution about 30 arc-second (0.93 kilometer) and triangular interpolated over the grid domain.

Open boundary condition

The open boundary is forced by water level from the harmonic analysis equation

$$\zeta(t) = A_0 + \sum_{i=1}^k A_i F_i \cos(\omega_i t + (V_0 + u)_i - G_i) \quad (5)$$

where A_0 is mean water level over a certain period (m), i is number of relevant constituents, k is index of a constituent, A_i is local tidal amplitude of a constituent (m), F_i is nodal amplitude factor, ω_i is angular velocity (deg/hr), $(V_0 + u)_i$ is

astronomical argument (deg) and G_i is improved kappa number.

The tidal constituents, including with 4 semi-diurnal components (M2, S2, N2 and K2), 4 diurnal components (K1, O1, P1 and Q1) and 5 longer period tides (M4, MS4, MN4, MF and MM) were derived from the harmonic analysis using a one year water

level prediction in 2014 at Ko Samui (SMT) and Laem Ngop (LGT) stations from the Hydrographic Department, Royal Thai Navy. These tidal constituent values of both stations are presented in Table 1. Along the open sea boundary, the linear interpolation of the astronomical constituents between two stations was implemented.

The Table 1. The tidal constituents at Ko Samui and Laem Ngop stations

Tidal constituents	Ko Samui				Laem Ngop			
	A _i (cm)	G _i (deg)	V _{0+u} (deg)	F	A _i (cm)	G _i (deg)	V _{0+u} (deg)	F
M2	16.2	310.9	211.8	1.0	10.9	31.6	211.8	1.0
S2	8.6	31.1	330.0	1.0	6.1	87.6	330.0	1.0
N2	2.7	269.9	5.1	1.0	2	6	5.1	1.0
K2	3.4	27.4	178.7	0.8	1.8	70.1	178.7	0.8
K1	36.5	176.7	359.7	0.9	44.8	152.3	359.7	0.9
O1	25.6	126.3	209.7	0.8	30.7	103.9	209.7	0.8
P1	5	170.8	334.6	1.0	12.8	150.9	334.6	1.0
Q1	0.8	105.4	3.1	0.8	5.7	82.1	3.1	0.8
M4	0.8	323.4	63.5	1.1	1.1	309	63.5	1.1
MS4	0.8	18	181.8	1.0	1.2	357	181.8	1.0
MN4	0.3	280	216.9	1.1	0.5	267.2	216.9	1.1
MF	1.3	9.9	332.3	0.7	0.7	13.1	332.3	0.7
MM	0.8	7.1	206.6	1.1	1.3	39.8	206.6	1.1

2.3 SWAN model

The SWAN model (Booij et al., 1999) is a third generation wave model that describes the evolution of wave over the sea from given wind, bottom, and current condition. The theoretical and numerical background of SWAN was presented in Holthuijsen et al. (1993), Ris et al. (1999), Booij et al. (1999), and Zijlema and Van der Westhuysen (2005).

The basic equation that is used in the SWAN model is action balance equation

$$\frac{\partial}{\partial t} N + \frac{\partial}{\partial x} c_x N + \frac{\partial}{\partial y} c_y N + \frac{\partial}{\partial \sigma} c_\sigma N + \frac{\partial}{\partial \theta} c_\theta N = \frac{S}{\sigma} \quad (6)$$

where $N = N(\sigma, \theta: x, y, t)$ is the action density as a function of radian frequency σ , direction θ , horizontal x , and y , and time t . The first term on the left-hand side represents the local rate of change of action density in time, the second and third terms represent propagation of action in geographical x, y space, respectively (with propagation velocities c_x and c_y). The fourth term represents shifting of the relative frequency due to variations in depths and

currents (with propagation velocity c_σ in σ space). The fifth term represents depth and current-induced refraction (with propagation velocity c_θ in θ space). The expressions for these propagation speeds are taken from linear wave theory. The term $S [= S(\sigma, \theta: x, y, t)]$ at the right-hand side of the action balance equation is a source term representing the effects of generation, dissipation, and nonlinear wave-wave interactions (Booij et al., 1999; Akpınar et al., 2012; Van der Westhuysen, 2002).

2.3.1 Model Setup

Grid domain

The rectangular grid of SWAN covers the Gulf of Thailand from a range of longitude 99° E to 105.5° E and latitude from 6° N to 14° N with 0.1 degree resolution (11.132 kilometer). The open sea boundary was assigned to be a straight line.

The bathymetry data were obtained and were interpolated from GEPCO resolution about 30 arc-second (0.93 kilometer).

The atmospheric forcing data used as principal input to the SWAN model in this study was the 6 hourly wind fields (four analyses fields per day, at 00, 06, 12, and 18 UTC) of the u and v wind components at 10 m from the ECMWF (European Centre for Medium-Range Weather Forecasts). In this study, the ECMWF ERA Interim data set was used because it is the latest version of the re-analyses and therefore it is considered to provide the most accurate data.

Open boundary condition

The wave data of significant wave height, peak period and peak direction were simulated in Global model by WAVEWATCH III spectral wave model which was developed at NOAA/NCEP (National Centers for Environmental Prediction).

3. Results and Discussions

The statistical analysis used to evaluate the performance of the model in this study is mean average error (MAE).

$$MAE = \frac{1}{N} \sum_{i=1}^N |X_i - Y_i| \quad (7)$$

where N is the amount of data, X_i is the water level of measured data and Y_i is the water level from model results.

3.1 Calibration and verification

3.1.1 Tidal current model

The sensitivity analysis of the physical parameters (roughness coefficient and eddy viscosity) in Delft3D modal was performed to check the sensitiveness of the model results due to changing of model parameters. In Table 2, those overall results were significantly sensitivity only to roughness coefficient.

For the calibration in January 2014, six constant Manning's n values of 0.016, 0.018, 0.020, 0.022, 0.024 and 0.026 were tested for this study. The results of simulated water level were compared with tide gauges (BBT, TCT, HHT and CPT) as represented in table 3. As evident from this table, Manning's n produced the lowest MAE is in the range of 0.022 to 0.024.

The period from 01/01/2013 – 31/12/2013 was used for verification process by comparing the result with prediction water level at 7 tide gauges from Hydrographic Department, Royal Thai Navy (SHT, SCT, BBT, TCT, HHT, KLT and CPT) as shown in Table 4. It was also found that pattern of water level from Delft3D showed a satisfactory agreement with the predicted data at all stations. The simulated water level from the model was overestimated about 0.10 to 0.25 m as shown in Fig. 2.

Table 2. The sensitivity tests of the physical parameters in Delft3D

Roughness	Viscosity	MAE (m)			
		BBT	TCT	HHT	CPT
0.01	5	0.290	0.459	0.195	0.260
0.02	5	0.201	0.433	0.153	0.267
0.03	5	0.216	0.423	0.188	0.269
0.03	1	0.238	0.423	0.188	0.269
0.03	5	0.238	0.423	0.188	0.269
0.03	10	0.238	0.423	0.188	0.269

Table 3. Calibration of Manning's n at tide gauges stations in January 2013

Manning's n	MAE (m)			
	BBT	TTC	HHT	CPT
0.016	0.238	0.441	0.164	0.266
0.018	0.222	0.436	0.157	0.267
0.020	0.209	0.433	0.153	0.267
0.022	0.200	0.430	0.153	0.267
0.024	0.197	0.428	0.156	0.267
0.026	0.200	0.426	0.161	0.268

Table 4. Verification of the water level at tide gauges stations.

Station	MAE (m)
SHT	0.090
SCT	0.172
BBT	0.178
TCT	0.262
HHT	0.127
KLT	0.112

CPT 0.103

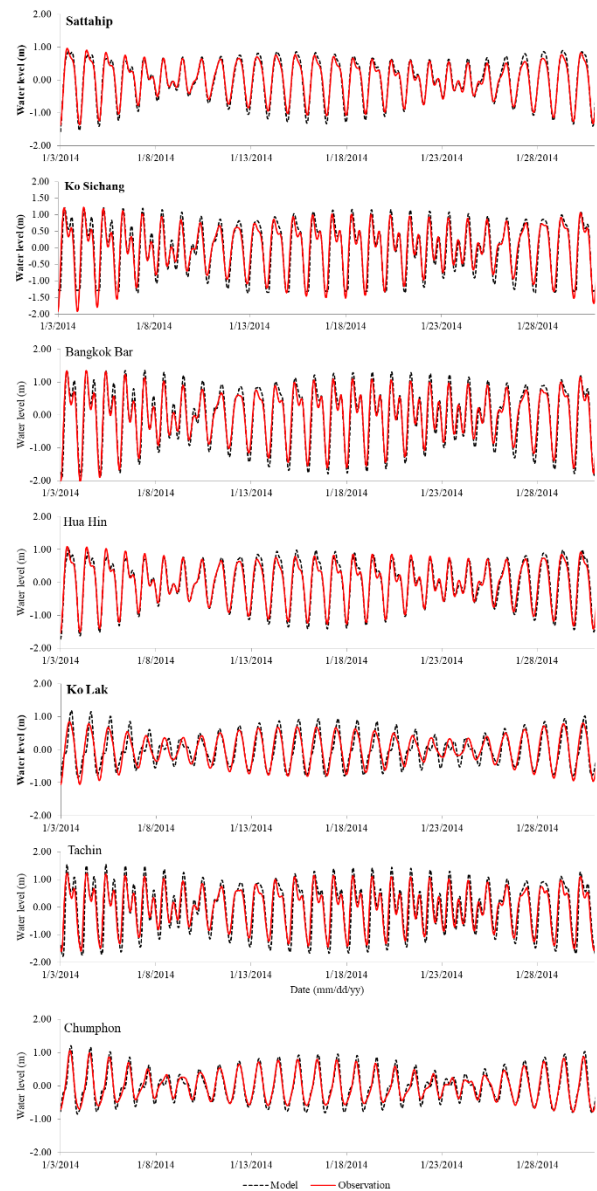


Fig. 2. Comparison of the water level between prediction and simulation.

3.1.2 Wind-Wave simulation

For the calibration of SWAN model, the significant wave height (H_s) and mean wave period (T) were the results compared with the observed data from 8 buoy stations. Four difference bottom friction formulations; i.e. Hasselmann et al. (1973) or JONSWAP, Collins (1972), Madsen et al. (1988), and Smith et al. (2001) were the test cases. The formation of bottom ripples and sediment size that the expression of Smith et al. (2001) with the specific

gravity of sediment 2.65 and the sediment size 0.0001 m was found the minimum errors based on the sensitivity studied of SWAN as shown in Table 5. Therefore, the Smith et al. (2001) expression was used for further simulations in this study.

Table 5. The sensitivity analysis of bottom friction formulations in SWAN model

Stations	MAE (m)			
	JON-SWAP	Collins	Madsen et al.	Smith et al.
KCB	0.116	0.116	0.114	0.095
RYB	0.054	0.054	0.054	0.055
SCB	0.055	0.055	0.054	0.059
HHB	0.041	0.041	0.042	0.050
PCB	0.052	0.052	0.051	0.067
KTB	0.104	0.104	0.104	0.089
NKB	0.117	0.117	0.117	0.097

To evaluate the SWAN model performance, a validation study was performed by comparing H_s with buoy observation data in nearshore during the Typhoon Linda in October 1997. The comparison of significant wave height between observed data and simulation results at 7 buoy stations (KCB, RYB, SCB, HHB, PCB, KTB, NKB) showed good result with small MAE values as presented in Table 6, and Fig. 3.

Table 6. Verification of SWAN model from 01/10/1997 – 31/10/1997

Stations	MAE (m)
KCB	0.116
RYB	0.054
SCB	0.055
HHB	0.042
PCB	0.052
KTB	0.104
NKB	0.117

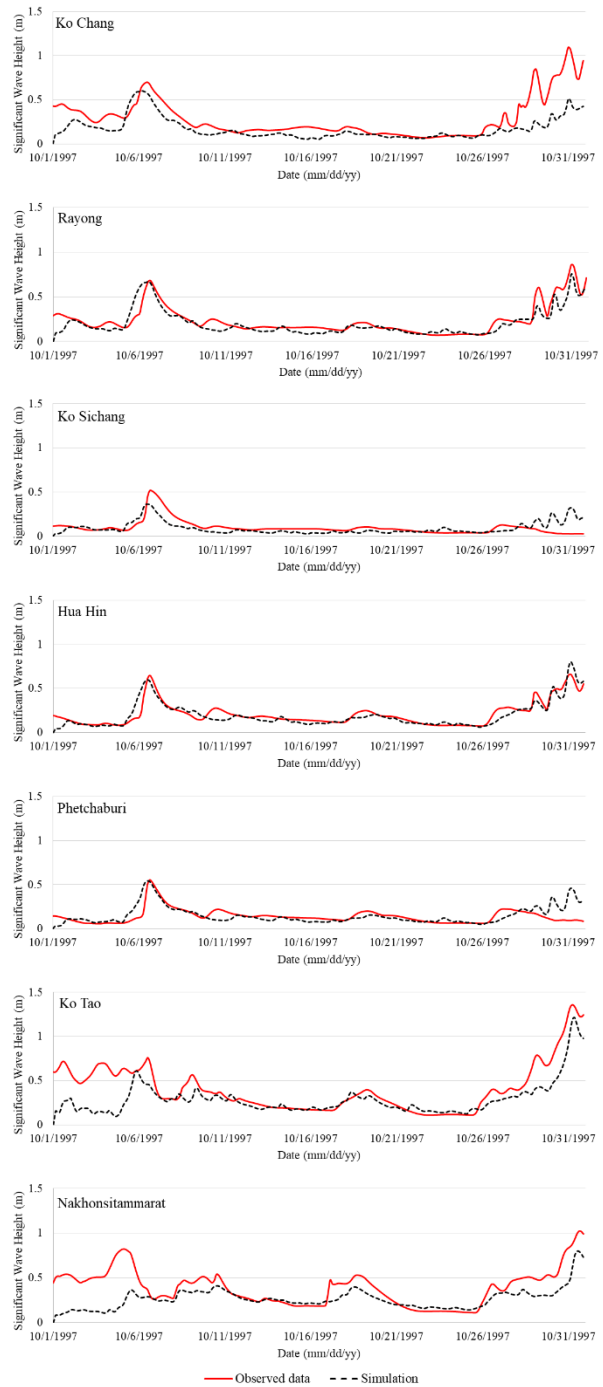


Fig. 3. Comparison of the significant wave height at 7 buoy stations.

3.1.3 Coupled wind-tidal model

For the coupled wind-tidal model, the values of water level and current were the key outputs from this model. Based on the available data, simulations was performed in 2013. Only the measured water level from the tide gauge of Port Authority of Thailand at Bangkok bar station was used for model verification.

The simulation results were divided into 4 groups of data from the meteorological condition of Thailand according to the monsoon regimes; i.e. December-February (Northeast Monsoon), March-May (First Inter-Monsoon), June-August (Southwest Monsoon) and September-November (Second Inter-Monsoon), and compared with the observed data as shown the MAE values in Table 7.

Table 7. Verification of coupled wind-tidal model in 2013.

Period	MAE (m)
Northeast Monsoon (NE)	0.28
First Inter-Monsoon	0.25
Southwest Monsoon (SW)	0.29
Second Inter-Monsoon	0.27

3.2 Simulation Results

After the tidal current model and the coupled wind-tidal model were calibrated and verified, the pattern of circulation in East Coast of the Gulf of Thailand from both models were simulated on the year 2013 as shown the result sample in Fig. 4a and 4b. Since the objective of this study was comparing the influence of wind and tidal to the circulation, the extraction of wind induced current was the necessary process. From the simulation results, there were currents in terms of u and v components of depth averaged velocity from both models. To extract the current from only wind, the simple subtraction of only tidal current from coupled wind-tidal current on each velocity components and computation grids was processed as shown in the sample result of only wind induced current in Fig. 4c. Finally, the only tidal, coupled wind-tidal and only wind currents were computed on every hour in year 2013.

3.3 Influence of wind and tidal on current

Actually, the circulation pattern in the sea was dominated by tidal and wind-wave. To identify the major effects on current, the influence of wind and tidal would be investigated in terms of magnitude and direction. To compute the effects on current magnitude, the tidal and wind influence parameters are introduced as presented in equation (8) and (9).

$$Tidal\ Influence = \frac{\|C_t\|}{\|C_t + C_w\|} \quad (8)$$

$$Wave\ Influence = 1 - Tidal\ Influence \quad (9)$$

where C_w , C_t and C_{w+t} are the vectors of wave, tidal and coupled wind-tidal current, respectively.

After the influence parameters were computed as shown in Table 8, it showed that all stations had the wind influence greater than the tidal influence. However, Maptaput and Chumporn stations still had the influence from both wind and tidal, since there were difference in the close gap between the values of wind and tidal influences.

Table 8. The influence of wind and tidal on current

Stations	Tidal Influence	Wind Influence
Maptaput	0.41	0.59
Sattahip	0.17	0.83
Bangkok Bar	0.16	0.84
Thachin	0.26	0.74
Hua Hin	0.20	0.80
Chumporn	0.46	0.54

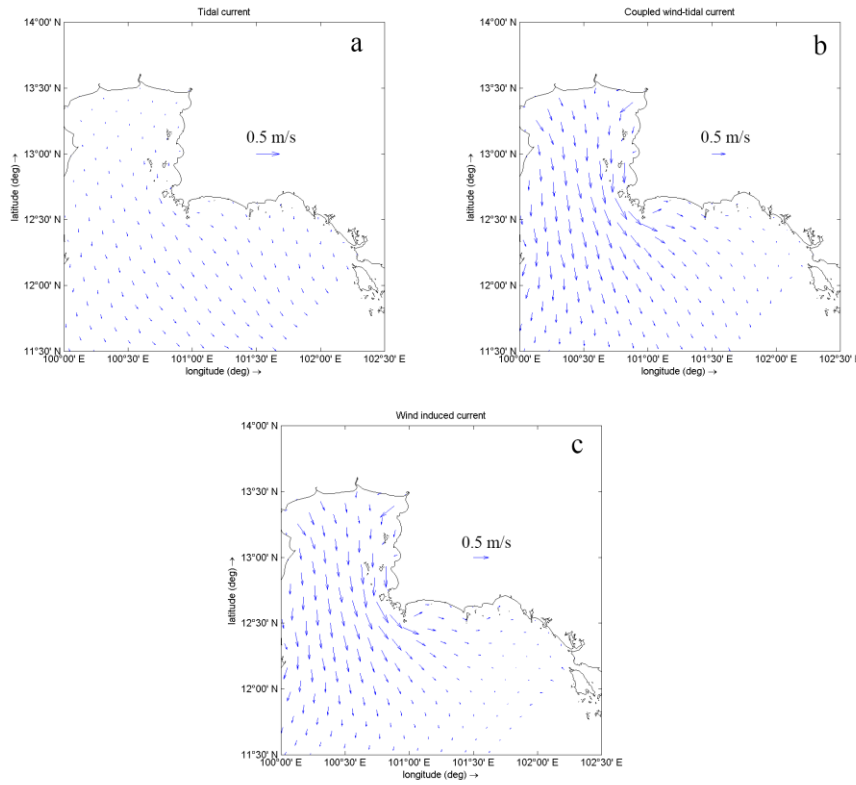


Fig. 4. Depth averaged velocity at 15 January 2013 (00:00) from a) the tidal current, b) the coupled wind-tidal current and c) the wind induced current.

Another property of current is its direction. To indicate current direction, the eight principal bearing used to measure current directions. The four cardinal points; i.e. north (N), south (S), east (E), and west (W), and the addition of the four intercardinal directions, northeast (NE) between north and east, southeast (SE), southwest (SW), and northwest (NW) were used for indicating the current direction according to equation (10). For comparing the direction from two sources of current, this study introduces the direction comparing parameter as presented in equation (11).

$$\theta = \begin{cases} N & ; 337.5 < \theta \leq 22.5 \\ NE & ; 22.5 < \theta \leq 67.5 \\ E & ; 67.5 < \theta \leq 112.5 \\ SE & ; 112.5 < \theta \leq 157.5 \\ S & ; 157.5 < \theta \leq 202.5 \\ SW & ; 202.5 < \theta \leq 247.5 \\ W & ; 247.5 < \theta \leq 292.5 \\ NW & ; 292.5 < \theta \leq 337.5 \end{cases} \quad (10)$$

$$\beta = \begin{cases} 0 & ; \theta_c \text{ and } \theta_{t,w} \text{ were same direction} \\ 1 & ; \theta_c \text{ and } \theta_{t,w} \text{ were } 45^\circ \text{ difference} \\ 2 & ; \theta_c \text{ and } \theta_{t,w} \text{ were } 90^\circ \text{ difference} \\ 3 & ; \theta_c \text{ and } \theta_{t,w} \text{ were } 135^\circ \text{ difference} \\ 4 & ; \theta_c \text{ and } \theta_{t,w} \text{ were opposite direction} \end{cases} \quad (11)$$

where β is the direction comparing parameters, θ_c is the direction of coupled wind-tidal current and $\theta_{t,w}$ is the direction of tidal or wind currents.

The percentage of the direction comparing parameters defined as

$$\% \beta_i = \frac{n_{\beta_i}}{N} \quad (12)$$

where n_{β} is the number of the direction comparing parameters, N is the total of data and i is index of relevant direction comparing parameters; i.e. β equal to 0, 1, 2, 3, and 4 respectively.

The percentage of the direction comparing parameters on tidal current to the coupled wind-tidal current are shown in Table 9. It can be seen that there was no relationship between these directions corresponding to the magnitude influence results.

On the other hand, the percentage of the direction comparing parameters on wind current to the coupled wind-tidal current as presented in Table 10. The results showed the same agreement with the magnitude influence parameters. The percentage of the direction comparing parameters in same direction ($\% \beta_0$) had the major ratio in almost stations. This could be implied that the influence of wind effects to the coupled wind-tidal more than the tidal. However, there were some uncertainties revealed as a slightly difference in direction at Maptaput and Chumporn stations. The most percentage of the direction comparing parameters of these 2 stations were $\% \beta_1$. This could be came from they got the influence from both wind and tidal which also shown in the magnitude influence parameter result.

Table 9. Percentage of the direction comparing parameters on tidal current to the coupled wind-tidal current

Stations	$\% \beta_0$	$\% \beta_1$	$\% \beta_2$	$\% \beta_3$	$\% \beta_4$
Maptaput	16.09	22.77	27.86	25.07	8.22
Sattahip	5.35	16.91	35.83	31.93	9.98
Bangkok Bar	38.46	5.98	3.21	6.29	46.05
Thachin	3.55	15.06	55.11	22.33	3.95
Hua Hin	43.15	4.55	1.02	1.80	49.48
Chumporn	15.49	32.34	25.92	18.93	7.32

Table 10. Percentage of the direction comparing parameters on wave current to the coupled wind-tidal current on direction

Stations	$\% \beta_0$	$\% \beta_1$	$\% \beta_2$	$\% \beta_3$	$\% \beta_4$
Maptaput	37.53	45.36	13.53	2.08	1.50
Sattahip	85.70	10.36	2.24	1.25	0.44
Bangkok Bar	91.68	6.29	1.06	0.65	0.32
Thachin	53.82	42.42	2.61	0.79	0.36
Hua Hin	85.90	9.38	1.49	1.51	1.73
Chumporn	27.53	47.52	17.29	5.08	2.58

4. Discussion and conclusion

The Delft3D is applied to compute tidal and wave current in Gulf of Thailand. A total of 13 constant tidal constituents based on the analysis and wave spectrum based on the simulation by SWAN model were applied along the open sea boundary. A simulation was made and the results were compared to the predicted water level at RYT, SHT, SCT, BBT, TCT, HHT, KLT and CPT stations, and the observed the significant wave height at KCB, RYB, SCB, HHB, PCB, CPB, KTB and NKB buoy stations. It was found that the model gives satisfactory results for both water levels and wave height.

Wind is the major effect to the circulation in almost stations in the Upper Gulf of Thailand, while there were some areas that the circulation are influenced by both tidal and wind. This can be seen that there were still some uncertainties on the sources which dominated the current in the Upper Gulf of Thailand. Long term investigation on this issue is still require, since this study provided on the preliminary result on 2013.

Acknowledgement

We would like to thank the NOAA (General Bathymetric Chart of Oceans, GEBCO) for the providing the bathymetry data of the Gulf of Thailand, the Hydrographic Department, Royal Thai Navy for the providing the hourly predicted water level data at tide gauges along the coast of the Gulf, the GISTDA for the significant wave height at oceanographic buoy stations, the ECMWF (ERA-Interim) for the wind data and the Port Authority of Thailand for the measurements of water level at Bangkok Bar station.

The authors would like to thank Dr. Suriyan Saramul and Kachapond Chettanawanit at Department of Marine Science, Faculty of Science, Chulalongkorn University for sharing experiences with the Delft3D and SWAN models.

We would like also thank to Research Unit on Technology for Oil Spill and Contamination Management, Chulalongkorn University for their valuable support.

References

- 1) Akpınar, A., 2012. Wave modeling and wave energy potential determination in the Black Sea, PhD Thesis last progressive report, Karadeniz Technical University, The Graduate School of Natural and Applied Sciences, Trabzon, Turkey.
- 2) Battjes, J.A., Janssen, J.P.F.M., 1978. Energy loss and set-up due to breaking of random waves. In: Proceedings of 16th International Conference on Coastal Engineering, ASCE, pp. 569–587.
- 3) Booij, N., Holthuijsen, L.H., Ris, R.C., 1999. A third-generation wave model for coastal regions. 1 Model description and validation. *Journal of Geophysical Research* 104 (C4), 7649–7666.
- 4) Buranpratheprat, A. and Bunpapong, M., 1998. Two Dimensional Hydrodynamic model for the Gulf of Thailand. Proceeding of the IOC/WESTPAC Fourth International Scientific Symposium, Okinawa, Japan. pp. 469-656.
- 5) Choi, B. H., Kim, D. G., and Kim, D. H., 1996. A numerical tidal model for the Southeast Asian sea. In Oil Spill modeling in the East Asian Region, Proceeding of the Regional Workshop on Oil Spill Modelling. Pusan, Republic of Korea, pp. 38-53.
- 6) Collins, J.I., 1972. Prediction of shallow water spectra. *Journal of Geophysical Research* 77 (15), 2693–2707.
- 7) Deltares., 2014. Delft3D-FLOW User Manual. 3.15 ed. MH Delft, Netherlands.
- 8) Department of Mineral Resources, 2012. Physical geology of the upper Gulf of Thailand. No.9/2012. Bureau of Geotechnology, Thailand.
- 9) Hasselmann, K., Barnett, T.P., Bouws, E., Carlson, H., Cartwright, D.E., Enke, K., Ewing, J.A., Gienapp, H., Hasselmann, D.E., Kruseman, P., Meerburg, A., Miller, P., Olbers, D.J., Richter, K., Sell, W., Walden, H., 1973. Measurements of wind- wave growth and swell decay during the Joint North Sea Wave Project (JONSWAP), *Ergänzungsheft zur Deutschen Hydrographischen Zeitschrift Reihe. Deutsches Hydrographisches Institute, Hamburg, Germany* 95pp.
- 10) Holthuijsen, L.H., Booij, N., Ris, R.C., 1993. A spectral wave model for the coastal zone. In: Proceedings 2nd International Symposium on Ocean Wave Measurement and Analysis, New Orleans, Louisiana, July 25–28, New York, pp. 630–641.
- 11) Komen, G.J., Hasselmann, S., Hasselmann, K., 1984. On the existence of a fully developed windsea spectrum. *Journal of Physical Oceanography* 14, 1271–1285.
- 12) Madsen, O.S., Poon, Y.K., Graber, H.C., 1988. Spectral wave attenuation by bottom friction: theory. In: Proceedings of 21st International Conference on Coastal Engineering, ASCE, pp. 492–504.

- 13) Pollution Control Department, 2010. Predictions for the movement of oil spill in the sea: Impact on natural resources and management solutions. Kotchakorn Publishing Limited Partnership, Bangkok.
- 14) Ris, R.C., Holthuijsen, L.H., Booij, N., 1999. A third-generation wave model for coastal regions: 2 Verification. *Journal of Geophysical Research* 104 (C4), 7667–7681.
- 15) Robinson, M. K., 1974. The physical oceanography of the Gulf of Thailand, Naga Expedition. In: NAGA Report Volume 3: Scientific Results of Marine Investigations of the South China Sea and the Gulf of Thailand 1959-1961. The University of California, Scripps Institution of Oceanography, La Jolla, California.
- 16) Siripong, A., 1984. Surface circulation in the Gulf of Thailand and South China Sea in 4 seasons from direct measurement. In *Proceeding of the Third Seminar on the Water Quality and the Quality of the Living Resource in Thai Waters*. Srinakharinwirot University, Chonburi. pp. 140-148.
- 17) Smith, J.M., Sherlock, A.R., Resio, D.T., 2001. STWAVE: Steady-State Spectral Wave Model User's Manual for STWAVE, Version 3.0. USACE, Engineer Research and Development Center. Technical Report ERDC/CHL SR-01-1, Vicksburg, MS.
- 18) The Hydrographic Department, 1995. Analysis of Oceanographic data in the Central Gulf of Thailand in 1982 – 1993. Royal Thai Navy.
- 19) Van der Westhuysen, A.J., 2002. The application of the numerical wind-wave model SWAN to a selected field case on the South African Coast. M.Sc. Thesis, the University of Stellenbosch, South Africa, 198 pp.
- 20) Yanagi, T., Takao, T. and Morimoto, A., 1997. Co-tidal and co-range charts in the South China Sea derived from satellite altimetry data. *La mer* 35: 85-93.
- 21) Yanagi, T. and T. Takao., 1998. Seasonal variation of three-dimensional circulations in the Gulf of Thailand. *La mer* 36: 43-55.
- 22) Zijlema, M., Van der Westhuysen, A.J., 2005. On convergence behaviour and numerical accuracy in stationary SWAN simulations of nearshore wind wave spectra. *Coastal Engineering* 52 (3), 237–256.